Article

Developmental Cell

A bHLH-Based Feedback Loop Restricts Vascular Cell Proliferation in Plants

Graphical Abstract

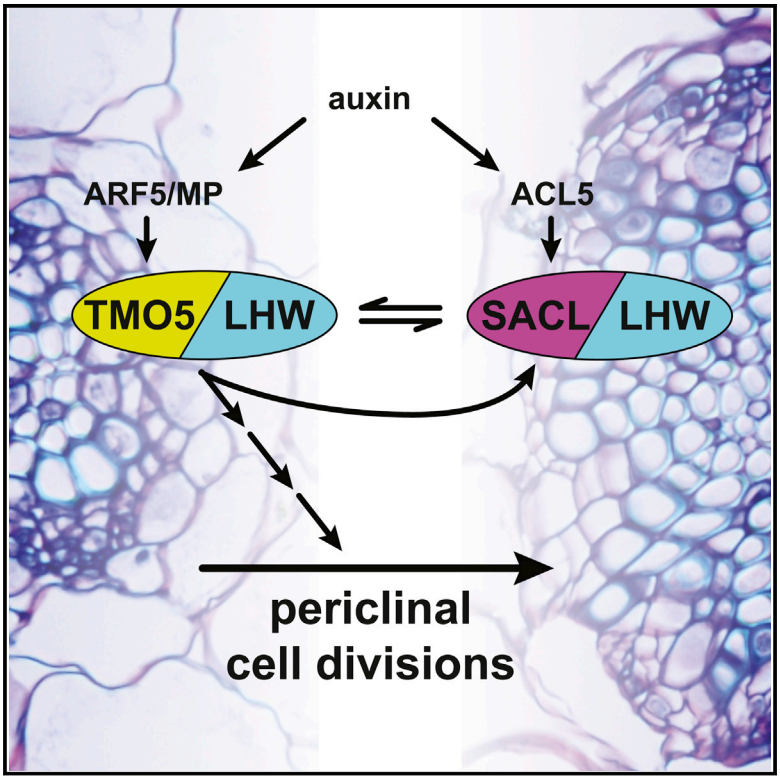

Authors

Francisco Vera-Sirera, Bert De Rybel, Cristina Úrbez, ..., Jan Willem Borst, Dolf Weijers, Miguel A. Blázquez

Correspondence

dolf.weijers@wur.nl (D.W.), mblazquez@ibmcp.upv.es (M.A.B.)

In Brief

Vera-Sirera, De Rybel et al. show that the correct number of cells in plant vasculature is established by the interplay between two opposing sets of bHLH transcription factors induced by the same hormone signals.

Highlights

- Increased activity of the TMO5/LHW complex causes excessive vascular cell divisions
- Thermospermine-regulated SACL proteins counteract the induction of TMO5/LHW targets
- Interaction with SACL proteins limits the activity of the TMO5/LHW complex
- Auxin adjusts vascular cell divisions through coordinated activation of SACL and TMO5

Accession Numbers

GSE70157

Vera-Sirera et al., 2015, Developmental Cell *35*, 432–443
November 23, 2015 ©2015 Elsevier Inc.
http://dx.doi.org/10.1016/j.devcel.2015.10.022

CellPress

Developmental Cell
Article

A bHLH-Based Feedback Loop Restricts Vascular Cell Proliferation in Plants

Francisco Vera-Sirera,[1,5] Bert De Rybel,[2,5,6] Cristina Úrbez,[1] Evangelos Kouklas,[2,7] Marta Pesquera,[1] Juan Camilo Álvarez-Mahecha,[1] Eugenio G. Minguet,[1] Hannele Tuominen,[3] Juan Carbonell,[1] Jan Willem Borst,[2,4] Dolf Weijers,[2,*] and Miguel A. Blázquez[1,*]

[1]Instituto de Biología Molecular y Celular de Plantas, Consejo Superior de Investigaciones Científicas-Universidad Politécnica de Valencia, 46022 Valencia, Spain

[2]Laboratory of Biochemistry, Wageningen University, Dreijenlaan 3, 6703 Wageningen, the Netherlands

[3]Umeå Plant Science Centre, Department of Plant Physiology, Umeå University, 90187 Umeå, Sweden

[4]Microspectroscopy Center, Wageningen University, Dreijenlaan 3, 6703 Wageningen, the Netherlands

[5]Co-first author

[6]Present address: Department of Plant Systems Biology, VIB, and Department of Plant Biotechnology and Bioinformatics, Ghent University, 9052 Ghent, Belgium

[7]Present address: Max Planck Institute for Plant Breeding Research, Carl-von-Linné-Weg 10, 50829 Köln, Germany

*Correspondence: dolf.weijers@wur.nl (D.W.), mblazquez@ibmcp.upv.es (M.A.B.)

http://dx.doi.org/10.1016/j.devcel.2015.10.022

SUMMARY

Control of tissue dimensions in multicellular organisms requires the precise quantitative regulation of mitotic activity. In plants, where cells are immobile, tissue size is achieved through control of both cell division orientation and mitotic rate. The bHLH transcription factor heterodimer formed by TARGET OF MONOPTEROS5 (TMO5) and LONESOME HIGHWAY (LHW) is a central regulator of vascular width-increasing divisions. An important unanswered question is how its activity is limited to specify vascular tissue dimensions. Here we identify a regulatory network that restricts TMO5/LHW activity. We show that thermospermine synthase ACAULIS5 antagonizes TMO5/LHW activity by promoting the accumulation of SAC51-LIKE (SACL) bHLH transcription factors. SACL proteins heterodimerize with LHW—therefore likely competing with TMO5/LHW interactions—prevent activation of TMO5/LHW target genes, and suppress the over-proliferation caused by excess TMO5/LHW activity. These findings connect two thus-far disparate pathways and provide a mechanistic understanding of the quantitative control of vascular tissue growth.

INTRODUCTION

Plant vascular tissues have essential but complex functions. In addition to mediating the transport of solutes, these tissues provide mechanical strength and stiffness (Lucas et al., 2013). Both of these functions depend on the number of vascular elements (strands, bundles) as well as on the size of each of these elements. In plants, tissue dimensions are regulated to a large degree through orientation of cell divisions. Because most plant organs, including the root and stem, elongate by the addition of new cells at the apical meristems, divisions that add cell files in the radial dimension (periclinal cell divisions) define tissue width. Therefore, periclinal divisions in meristems are a key determinant for the width of vascular tissues in primary growth. Similarly, secondary growth of the vascular tissues (e.g., during wood formation) (Jouannet et al., 2015; Nieminen et al., 2015) is equally driven by oriented, periclinal divisions that add cells in the radial dimension.

Several genetic regulators have been shown to promote periclinal cell division and, therefore, radial growth of the vascular tissues. The cytokinin (CK) hormone response pathway is critically required for periclinal cell division in the vascular lineage because mutations in the CK receptors, including *ARABIDOPSIS HISTIDINE KINASE 4/CYTOKININ RESPONSE 1* (*AHK4/CRE1*), or in the *LONELY GUY* (*LOG*) CK biosynthetic genes cause a dramatic reduction in vascular tissue width (Mähönen et al., 2000, 2006; Tokunaga et al., 2012). Furthermore, the auxin-regulated bHLH transcription factor TARGET OF MONOPTEROS5 (TMO5) and its heterodimeric basic helix-loop-helix (bHLH) partner LONESOME HIGHWAY (LHW), as well as their respective homologs, are both necessary and sufficient for promoting periclinal divisions in the vascular lineage. The obligate requirement for the presence of TMO5 and LHW in the complex is evident in that loss of either one of the partners causes a strong decrease in the number of vascular cell files, whereas combined misexpression of both causes ectopic periclinal divisions and an excess of cell files within and outside of the vascular tissues (De Rybel et al., 2013; Ohashi-Ito and Bergmann, 2007; Ohashi-Ito et al., 2013). Recently, the CK and TMO5/LHW components were connected; analysis of direct transcriptional targets of the TMO5/LHW dimer revealed that these transcription factors act through promoting CK biosynthesis (De Rybel et al., 2014; Ohashi-Ito et al., 2014).

These results indicate that this pathway is important for promoting vascular periclinal divisions, but the dramatic effects of TMO5/LHW misexpression also demonstrate that the activity of this transcription complex must be kept in check. An important question, therefore, is how the activity of this complex is limited to the small zone of the vascular meristem where periclinal divisions occur.

There have not been many reports of mutants with excessive vascular tissue size, but mutations in the *ACAULIS5* (*ACL5*) gene have been shown to induce over-proliferation of xylem vessel elements in vascular bundles of inflorescence stems (Hanzawa et al., 1997). This increase in vascular tissue size is accompanied by severely dwarfed growth of the plant (Hanzawa et al., 1997). At present, it is unclear how the ACL5 enzyme, which catalyzes thermospermine biosynthesis (Knott et al., 2007), acts to limit vascular tissue proliferation. A genetic screen for suppressors of the dwarf phenotype of the *acl5* mutant identified multiple components involved in translation (RPL4, RPL10, and RACK1) (Kakehi et al., 2015; Imai et al., 2008) as well as SUPPRESSOR OF ACAULIS 51 (SAC51) (Imai et al., 2006), a bHLH transcription factor whose accumulation seems to be promoted by thermospermine through a still unidentified mechanism (Takano et al., 2012). Despite the involvement of ACL5/SAC51 in vascular development, it is not known how this regulatory module connects to other components in vascular tissue growth, such as the TMO5/LHW-CK pathway.

Here we identify the SAC51-LIKE (SACL) clade, composed of SAC51 and three SAC51-like bHLH transcription factors, as important negative regulators of the TMO5/LHW dimer. We show that TMO5/LHW activates the transcription of *SACL* genes and, therefore, activates a feedback mechanism that limits the promoting vascular periclinal division activity. These results link two so far unconnected pathways and provide a mechanism for the quantitative control of vascular proliferation.

RESULTS

ACL5 Antagonizes TMO5/LHW Function in Controlling Vascular Cell Divisions

The post-embryonic phenotype of plants overexpressing *TMO5* and *LHW* includes not only an excess of vascular cell files in roots (De Rybel et al., 2013; Ohashi-Ito et al., 2014) but also a remarkable increase in cell division within leaf veins and the vascular cylinder of the hypocotyl (Figures 1A–1D). This defect resembles the reported "thickvein" phenotype and the over-proliferation of vascular cells in stems and young hypocotyls caused by loss of ACL5 function (Clay and Nelson, 2005; Hanzawa et al., 1997), and, although with different architectures, the stature of both *TMO5/LHW* overexpressors and *acl5* mutant plants is shorter than that of the wild-type (Figure S1). The possibility of a functional connection between ACL5 and TMO5/LHW was investigated by an in silico meta-analysis of published transcriptomes for *acl5* mutants (Tong et al., 2014), *TMO5* induction (De Rybel et al., 2014), and *T5L1/LHW* induction (Ohashi-Ito et al., 2014). Despite the very different tissues and experimental conditions under which the transcriptomes were obtained, there was a set of 16 genes upregulated in *acl5* and under at least one of the other two conditions (Figure 1E). Included are transcription factors associated with vascular development (such as ATHB8, TMO5, and TMO5-LIKE1) and, notably, the CK biosynthesis enzyme LOG4, which promotes cell divisions in the shoot apical meristem (Chickarmane et al., 2012) and in developing vascular cells (De Rybel et al., 2014; Ohashi-Ito et al., 2014). Consistent with the enhanced expression of the cytokinin biosynthesis gene *LOG4*, several cytokinin-regulated genes were upregulated in the *acl5* mutant (Figure 1F).

Given the upregulation of *LOG4* expression (Figure 1E), the role of ACL5 and LHW in the development of xylem (Muñiz et al., 2008; Ohashi-Ito et al., 2013), the overlapping expression domains of *ACL5* and *TMO5/LHW* in xylem cells (De Rybel et al., 2013; Muñiz et al., 2008), and the over-proliferation defects of vascular cells caused by both loss of *ACL5* and gain of *TMO5/LHW* function (Figures 1A–1D), it seems possible that ACL5 could serve as a control mechanism that prevents excessive TMO5/LHW activity. In that case, genetic reduction of TMO5/LHW dimer activity should alleviate the *acl5* deficient phenotype. Indeed, the severe impairment of stem elongation in *acl5* mutants (Hanzawa et al., 1997; Hanzawa et al., 2000) was partially suppressed in an *acl5 lhw* double mutant background (Figure 2A). Similarly, the increased number of vascular cells in *acl5* hypocotyls was reverted in the presence of the *lhw* mutation to wild-type levels (Figures 2B–2F). The epistasis of *LHW* over *ACL5* was also evident when examining vascular cell number in roots. The *lhw* mutant shows a reduced number of vascular cells, resulting in roots that present single phloem and xylem poles (Ohashi-Ito and Bergmann, 2007; Figures 2G and 2I). Contrary to this effect, we found an increase in the average number of xylem cells of *acl5* roots (Figures 2G and 2H), whereas the double *acl5 lhw* mutant behaved as the single *lhw* mutant (Figures 2G–2K). These results indicate that the *acl5*-dependent vascular cell over-proliferation throughout the plant depends on LHW activity. Consistent with this, we confirmed that the overlap between ACL5 and TMO5/LHW targets revealed by transcriptomic meta-analysis, in fact, reflected a functional connection because the upregulation of *LOG4* and at least two additional targets observed in *acl5* was largely reverted in the *acl5 lhw* double mutant (Figures 2L–2N).

Translational Regulation of AJAX/SACL bHLH Proteins Controls Vascular Cell Division

The identity of ACL5 as a thermospermine synthase (Knott et al., 2007) does not provide an immediate molecular mechanism by which it would limit TMO5/LHW activity. To identify possible elements downstream of ACL5 that would act as regulators of TMO5/LHW, we screened for extragenic mutations that would suppress the *acl5* short stem phenotype (see Experimental Procedures for details). Ten dominant mutants were isolated in the M1 generation that displayed a reverted high stature and were named *ajax*. As expected, not only was stem elongation restored in the *acl5 ajax* double mutants (Figure 3A), but, also, the vascular cell over-proliferation defects in the hypocotyl (Figures 3B and 3C), leaves (Figures 3D and 3E), and roots (Figure S2) were largely corrected by the presence of *ajax* mutations.

Positional cloning of *ajax1-14* and *ajax2-31* revealed that these mutations affect an upstream open reading frame (uORF) in the 5′ UTR of At5g64340 (*AJAX1*) and At1g29950 (*AJAX2*), respectively, encoding two members of group XIV bHLH family transcription factors (Toledo-Ortiz et al., 2003; Figure S3). *AJAX1* is allelic to *SAC51*, a previously reported suppressor of *acl5* (Imai et al., 2006), and *AJAX2* was previously named *SACL3* (Kakehi et al., 2010). Therefore, from now on, we will refer to these genes as *SAC51* and *SACL3*. A distinctive attribute of the four members of this clade is the presence of a long 5′ UTR with small uORFs (Figure S3), which, at least in the case of *SAC51*, has been shown to negatively modulate the translation of the main ORF (Imai

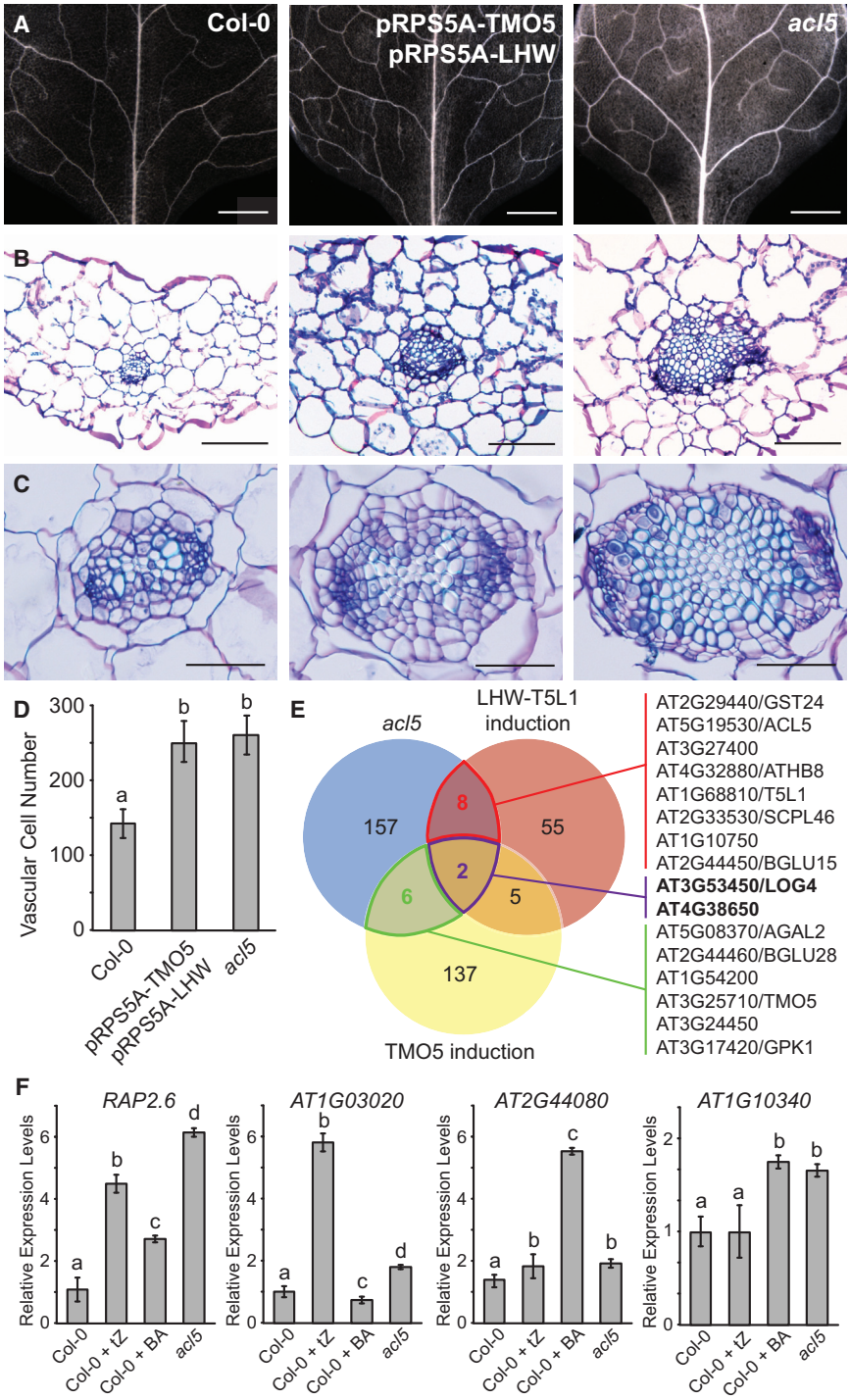

Figure 1. Overexpression of *TMO5* and *LHW* Resembles Loss of *ACL5* Function

(A and B) *TMO5/LHW* overexpressors display the "thickvein" phenotype characteristic of the *acl5* mutant (Clay and Nelson, 2005). Scale bars, 100 μm.

(A) The third true leaf of Col-0, *acl5*, and pRPS5A-*TMO5* pRPS5A-*LHW* was selected and cleared with chloral hydrate.

(B) Sections across the main vein of the third true leaf of the same genotypes.

(C) Representative sections across 12-day-old hypocotyls. Scale bars, 100 μm.

(D) Number of cells within the hypocotyl vascular cylinders of 12-day-old seedlings. Means ± SD are represented, and different letters show significantly different means (Tukey's HSD, $p < 0.05$).

(E) Overlap between the sets of misregulated genes in *acl5* 7-day-old seedlings (blue) (Tong et al., 2014), *Arabidopsis* culture cells after conditional induction of *LHW-T5L1* (red) (Ohashi-Ito et al., 2014), and roots of 4-day-old seedling *TMO5* induction (yellow) (De Rybel et al., 2014). The 16 common genes between *acl5* set and the other two sets are indicated.

(F) Four CK-responsive genes were also upregulated in *acl5*. Expression was analyzed by qRT-PCR in 7-day-old seedlings treated with either 0.5 μM *trans*-zeatin (tZ) for 16 hr or with 10 μM benzyladenine (BA) for 2 hr. Means ± SD are represented, and different letters show significantly different means (Tukey's HSD, $p < 0.05$).

et al., 2006). We sequenced the genomic loci of *SAC51*, *SACL3*, and the two closely related genes At5g09460 (*AJAX3/SACL1*) and At5g50010 (*SACL2*) (Kakehi et al., 2010) in the remaining *ajax* mutants and found that they all contained point mutations in the equivalent uORFs in *SAC51*, *SACL3*, and *SACL1* but not in *SACL2* (Figure 3F). Interestingly, three of the ten new alleles generated a stop codon in the predicted sequence of the uORF, similar to the *sac51-d* mutant (Imai et al., 2006). All other alleles represented amino acid substitutions in conserved positions of the uORF (Figure 3F), suggesting that translational control by the uORF might rely on the biological activity of the encoded peptide, which could act as a negative regulator of the *SACL* main ORF translation.

Two pieces of evidence confirmed that the dominant nature of the *ajax* alleles was caused by increased translation of the main ORF encoding the *SACL* bHLH transcription factor. First, constitutive expression of only the main ORF of *SACL3* restored the wild-type phenotype in *acl5* mutant plants (Figure 3G). Second, an in vitro transcription-translation assay using chimeric *SACL3* mRNAs in wheat germ extracts indicated that the main ORF was only translated when no small uORF preceded the main ORF or when the preceding small uORF contained missense or nonsense mutations (Figure 3H).

SACL Proteins Are Direct Inhibitors of LHW Activity

Given that the over-proliferation of vascular cells and other associated defects observed in *acl5* are suppressed by gain-of-function mutations in *SACL* genes, we hypothesized that the SACL proteins are necessary to control cell division during vascular

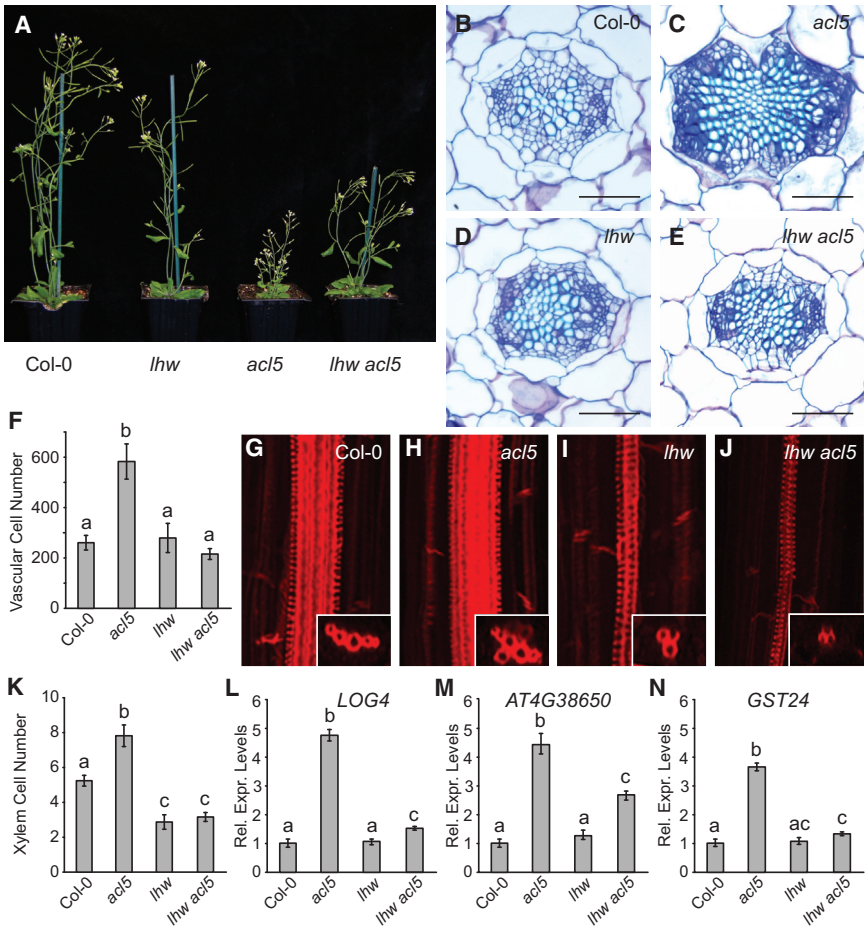

Figure 2. Loss of LHW Function Suppresses the Vasculature-Related Defects of *acl5*

(A) The dwarfism caused by *acl5* is partially suppressed by *lhw*. Shown are pictures of representative individuals of each genotype.

(B–E) Representative sections across the hypocotyl of 12-day-old wild-type (B), *acl5* (C), *lhw* (D), and *lhw acl5* (E) seedlings. Scale bars, 100 μm.

(F) Number of cells within the vascular cylinder of the hypocotyls of 12-day-old seedlings. Means ± SD are represented, and different letters show significantly different means (Tukey's HSD, $p < 0.05$).

(G–J) Suppression by *lhw* of the over-proliferation of root vascular cells in *acl5*. Representative images of wild-type (G), *acl5* (H), *lhw* (I), and *lhw acl5* (J) roots are shown after basic fuchsin staining of 4-day-old seedlings. Images were taken 0.75 mm below the hypocotyl-root junction.

(K) Values represent the average of xylem cells ± SD, and different letters show significantly different means (Tukey's HSD, $p < 0.05$).

(L–N) The upregulation in *acl5* of three putative target genes is suppressed by *lhw*. The graphs correspond to a single representative experiment. Means ± SD are represented, and different letters show significantly different means (Tukey's HSD, $p < 0.05$).

development, probably by restricting activity of the TMO5/LHW complex.

To investigate this hypothesis, we first examined the extent of the overlap in the gene expression domains of *TMO5*, *LHW*, and *SACL* genes. *TMO5* and its homologs are expressed in young xylem cells of the root meristem, whereas *LHW* and its homologs are more broadly expressed (De Rybel et al., 2013; Ohashi-Ito and Bergmann, 2007; Ohashi-Ito et al., 2013). Accordingly, transcriptional reporters for all four *SACL* genes expressing a triple nuclear GFP under the control of the corresponding promoters (p*SACL::n3GFP*) displayed vascular-specific accumulation in the root (Figures 4A–4D). Deletion of the uORF (p*SACL*ΔuORF::n3GFP) did not change the expression domains, and only the intensity of GFP fluorescence increased, possibly because translational repression by the uORF had been eliminated (Figures 4E–4H). The enhanced expression in these lines also allowed a more precise analysis of gene expression patterns. Although *SAC51* is more broadly expressed within the vascular cylinder (Figures 4A and 4E), *SACL1* expression is restricted to the protophloem poles (Figures 4B and 4F), *SACL2* expression marks cambial cells (Figures 4C and 4G), and *SACL3* is expressed in xylem and pericycle (Figures 4D and 4H). Importantly, exogenous application of thermospermine to the pSACL::n3GFP lines also caused an expansion of the expression domain of at least *SAC51*, *SACL1*, and *SACL3* (Figures S4A–S4H), suggesting that the accumulation pattern of these SACL proteins is also established by the local availability of endogenous thermospermine.

The vascular-specific expression domains of *SACL*, *LHW*, and *TMO5* were also observed in aerial parts of the plant, such as hypocotyls (Figures S4I–S4N). Moreover, specifically *SACL3* was expressed during embryogenesis from the globular stage onward in provascular initial cells (Figures 4I and 4J), again overlapping with *TMO5* and *LHW* expression domains (De Rybel et al., 2013).

SACL proteins belong to the class of bHLH transcription factors that lack a well-defined basic domain required for DNA binding (Toledo-Ortiz et al., 2003). Their transcriptional regulation capacity, therefore, may rely on their interaction with other bHLH transcription factors. An immunoprecipitation followed by tandem mass spectrometry (IP-MS/MS) identified SAC51 and SACL3 (Table S1) as interacting in vivo with LHW (De Rybel et al., 2013), whereas, in vitro, interaction between SACL3 and LHW has also been shown previously in a yeast two-hybrid (Y2H) screening (Ohashi-Ito and Bergmann, 2007). These data strongly suggest that the SACL proteins directly interact with LHW, which we confirmed by Y2H for all SACL proteins (Figure 5A) and by Förster resonance energy transfer (FRET), measured by fluorescence lifetime imaging (FLIM) using SACL3-sCFP3A and LHW-sYFP2 fusion proteins expressed in a transient *Arabidopsis* leaf mesophyll protoplast system (Figure 5B).

Given the identity of the SACL proteins as bHLH transcription factors, we examined their presence in the nucleus using *Nicotiana benthamiana* leaves agroinfiltrated with constitutively expressed GFP-tagged versions of all four SACL proteins.

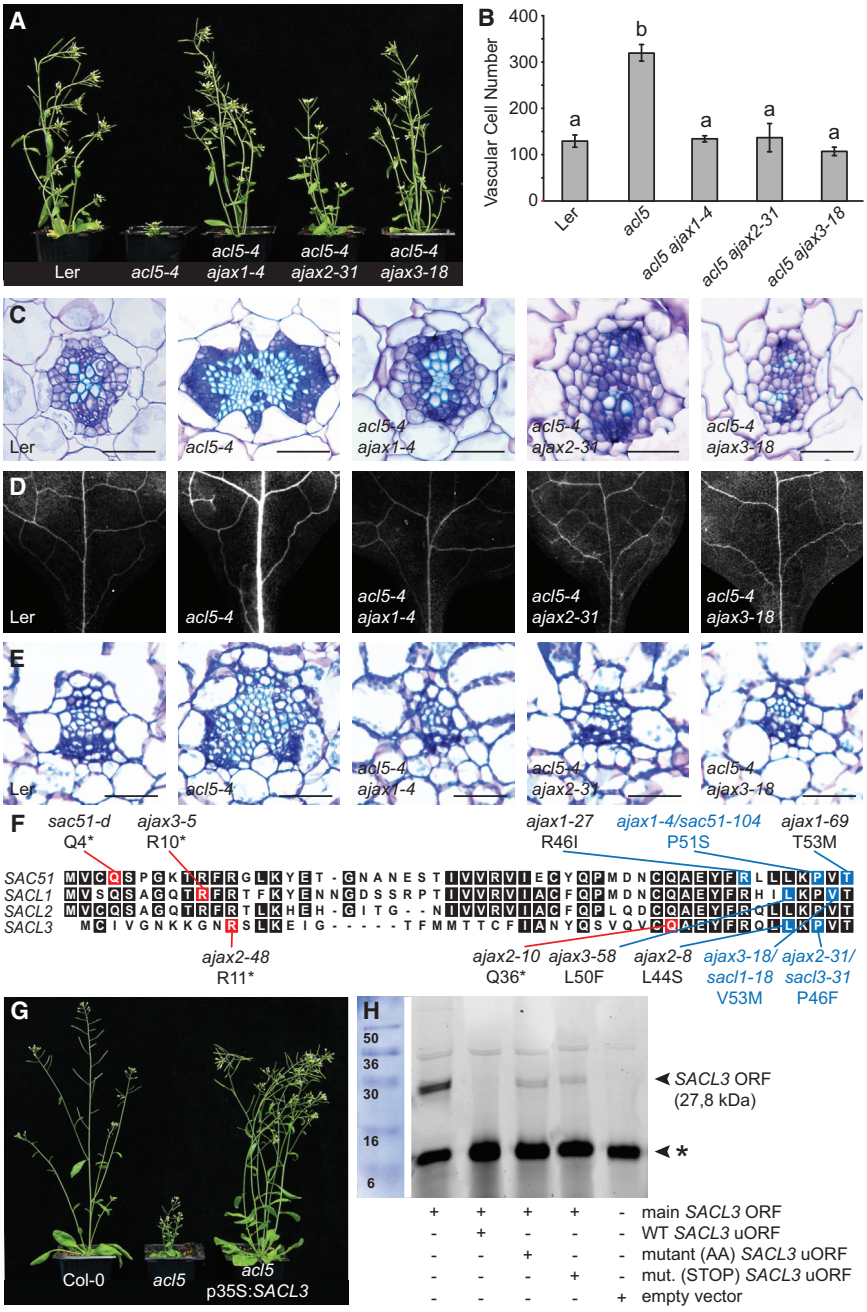

Figure 3. Dominant Mutations in *SACL* Genes Encoding bHLH Transcription Factors Suppress the Defects Caused by *acl5*

(A) Adult plant phenotype of representative *ajax* suppressors.

(B) Number of cells within the vascular cylinder of the hypocotyls of 12-day-old seedlings. Means ± SD are represented, and different letters show significantly different means (Tukey's HSD, $p < 0.05$).

(C) Representative sections of 12-day-old hypocotyls in which *ajax* mutations suppress the vascular cell over-proliferation caused by *acl5*. Scale bars, 100 μm.

(D and E) Representative images of the third leaf of the different genotypes after chloral hydrate clearing (D) and cross sections of the main vein in the same leaves (E). Scale bars, 100 μm.

(F) Conserved uORF peptides from the four *SACL* 5′ UTRs, indicating the mutant suppressing alleles. Black amino acids represent conserved positions, blue and red amino acids represent amino acid change mutations that suppress *acl5* mutant, blue ones are amino acid changes (new amino acid is indicated in brackets), and red ones are stop codons.

(G) Suppression of the *acl5* dwarfism by overexpression of the main *SACL3* ORF.

(H) An in vitro transcription-translation assay of the main *SACL3* ORF alone or including wild-type or mutant versions of the small uORF. The first lane corresponds to the Coomassie-stained ladder. The asterisk represents an unspecific band that served as a loading control.

Although SACL2-GFP could not be detected, all other SACL fusion proteins showed a nuclear localization (Figures 4K–4O). Interestingly, SACL3-GFP was also detected in the cytoplasm (Figure 4O), resembling the dual localization of LHW (Figure 4L; De Rybel et al., 2013). Because of the nuclear localization of SACL proteins in this system, further *Nicotiana benthamiana* transient expression assays were performed to test the effect of SACL3 on the transcriptional activity of LHW using firefly luciferase under the control of the *LOG4* promoter (p*LOG4*::LUC) as a reporter. As expected from the ability of LHW to bind the *LOG4* promoter (De Rybel et al., 2014; Ohashi-Ito et al., 2014), agroinfiltration of LHW induced expression of the *LOG4* reporter, and this effect was enhanced by TMO5 (Figure 5C). However, co-infiltration of increasing doses of SACL3 gradually reduced the ability of LHW to upregulate the *LOG4* reporter (Figure 5C). Vice versa, increasing doses of TMO5 gradually alleviated inhibition of LHW by SACL3 (Figure 5C). These results suggest that SACL proteins not only bind LHW directly but that they are also able to inhibit TMO5/LHW activity.

TMO5/LHW Activity Is Modulated by SACL Proteins In Vivo

To evaluate the effect of this inhibitory mechanism on TMO5/LHW activity in vivo, we decided to first identify molecular targets of SACL proteins and then examine them in the different genetic backgrounds. Given that the biological activity of SACL proteins is more clearly observed in the *acl5* mutant background, we constructed transgenic plants expressing the main ORF of the *SACL3* gene under the control of a heat shock-inducible promoter (Matsuhara et al., 2000) in *acl5* (pHS::*SACL3*) and subsequently determined transcript profiles (Table S2). According to the tests performed to examine the induction kinetics and the temporal accumulation pattern of the SACL3 protein (Figure S5A), a 30-min treatment at 37°C and two sampling times (1 and 4 hr after the beginning of the heat shock) were selected for transcript profiling and the

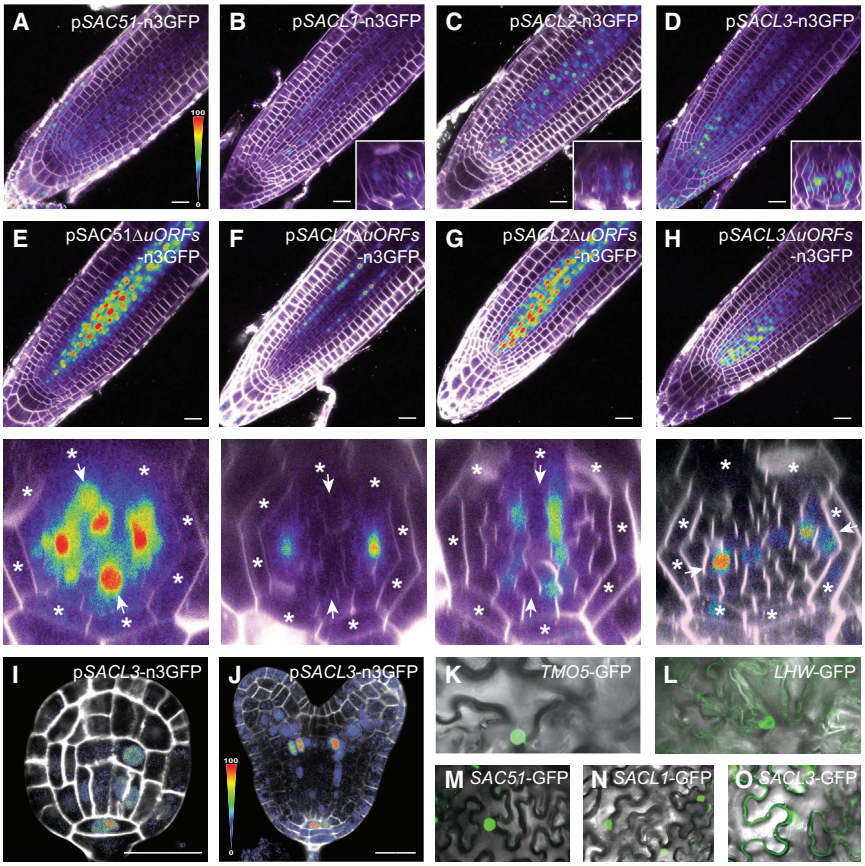

Figure 4. *SACL* Genes Show Vasculature-Specific Expression Patterns

(A–H) Expression of a nuclearly localized version of GFP in roots (n3GFP) driven by 3 kb of the promoters of the four *SACL* genes with (A–D) or without (E–H) the corresponding 5′ uORF. Optical transverse sections are shown below the corresponding longitudinal sections.

(I and J) GFP expression driven by the *SACL3* promoter in a late globular (I) and late heart stage (J) embryo.

(A–J) False colorscale images with the highest expression in red and lowest in blue. Scale bars, 20 μm. Asterisks indicate endodermal cells, and arrows indicate the xylem axis.

(K–O) Subcellular localization of constitutively expressed GFP-tagged versions of TMO5, LHW, and three SACL proteins after agroinfiltration in *Nicotiana benthamiana* leaves.

identification of putative primary targets of SACL3. A total of 614 differentially expressed genes were identified in the *acl5* mutant, of which only 1% were significantly corrected after 1 hr of SACL3 induction. The number of genes altered in *acl5* but restored to wild-type levels by SACL3 still increased to 6% after 4 hr and 47% in the *acl5 sacl3-31* (Figures S5C–S5E), indicating that short-time induction of SACL3 allows the identification of likely primary targets and that most of the transcriptional defects caused by loss of ACL5 function are due to reduced levels of SACL proteins. More importantly, among the putative primary targets of SACL3 were several genes involved in vascular development, including *LOG4* (Figure 5D). These results indicate that the SACL3 protein regulates relevant TMO5/LHW targets involved in vascular development in vivo. To confirm that increased SACL protein levels can suppress the defects caused by *TMO5/LHW* overexpression, we introduced the pHS::*SACL3* construct in a *TMO5/LHW* misexpression background (pRPS5A::*TMO5*/pRPS5A::*LHW*). Just as in the *acl5* mutant background, induction of SACL3 was able to reduce the expression levels of *LOG4* (Figure 6A).

To investigate the extent of the suppression by SACL proteins of *TMO5/LHW* overexpression with respect to vascular development, we analyzed hypocotyl (Figures 6B–6H) and root (Figure 6I) vascular anatomy in the same TMO5/LHW misexpression lines carrying pRPS5A::*SACL* constructs. As expected, overexpression of *SACL* genes was able to reduce the effect of excessive TMO5/LHW dimer activity (Figures 6B–6H), confirming that SACL proteins restrict TMO5/LHW activity in vivo to achieve proper cell division levels during vascular development.

In this model, overexpression of *SACL* genes should result in TMO5/LHW loss-of-function phenotypes. Indeed, overexpression of any of the four *SACL* genes (p35S::*SACL*) in a wild-type background resulted in a strong reduction in vascular cell divisions in the root (Figures 7A–7E) and a high proportion of individuals with monarch vascular patterns and loss of protoxylem (Figure S6), mimicking *t5-t5l1-t5l2-t5l3* quadruple or *lhw-ll1* double mutant phenotypes (De Rybel et al., 2013). A similar defect was found in the aerial parts of the p35S::*SACL* lines, resulting in defective venation patterns in cotyledons (Figure 7F) and severely dwarfed plants phenocopying the higher-order *tmo5* and *lhw* loss-of-function mutants (Figure S7). These combined data show that SACL proteins act as direct repressors of TMO5/LHW activity in vivo.

Intriguingly, previous microarray experiments have shown that *SACL* genes were potential targets of TMO5 (De Rybel et al., 2014), and we confirmed by qRT-PCR that *SACL1-3* was upregulated by dexamethasone in a TMO5-GR line even in the presence of cycloheximide (Figure 7G). The negative feedback loop formed in this way ensures that this intricate regulatory mechanism keeps TMO5/LHW activity in check, allowing normal vascular development (Figure 7H).

DISCUSSION

Because of their sessile nature and lack of cell mobility, plants have to rely on strictly controlled cell division orientation for proper three-dimensional growth and development. Particularly in organs with a defined main growth axis (roots, stems), divisions perpendicular to the axis (periclinal) can increase the width of the organ when these divisions occur in the meristematic tip. A key question, therefore, is how zones of periclinal division

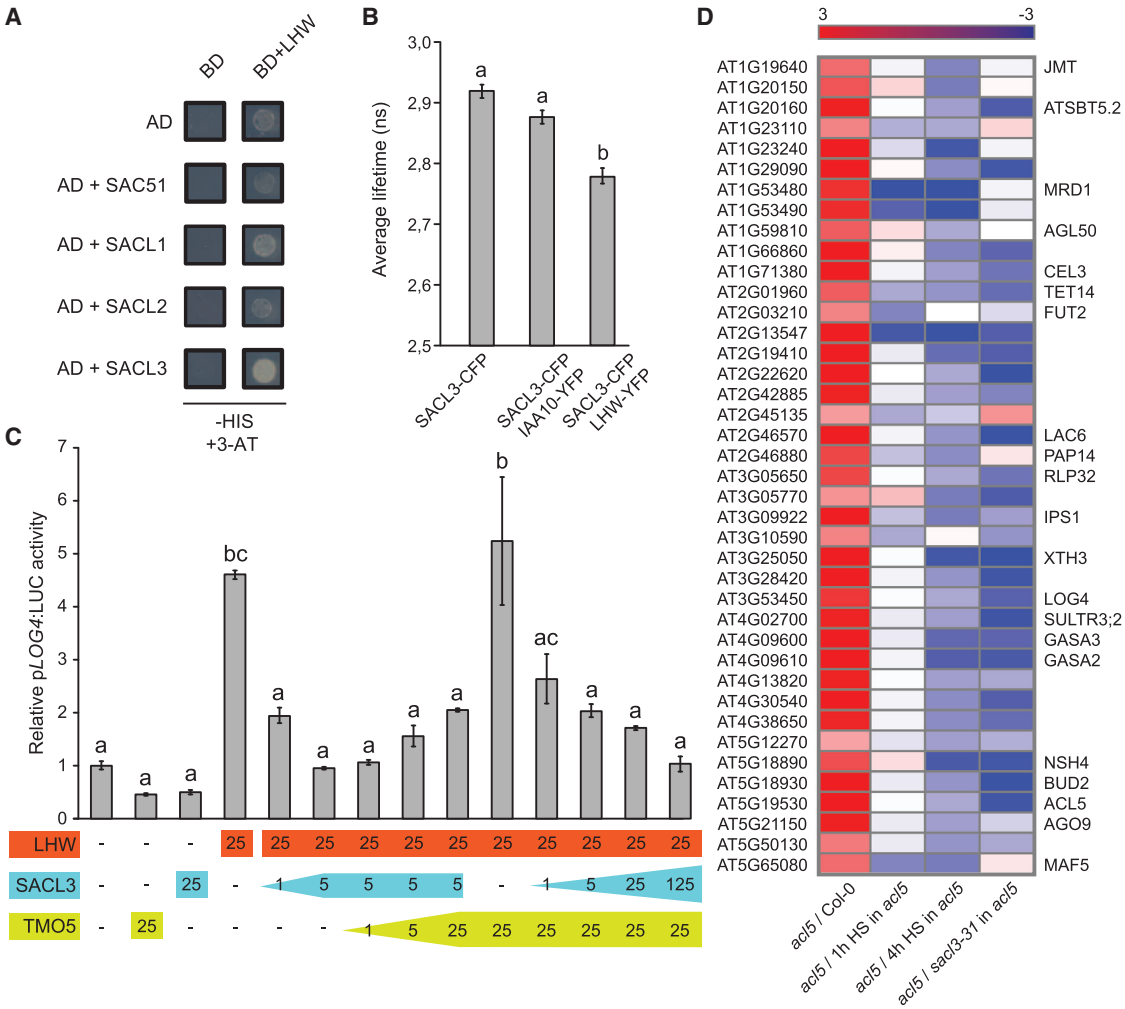

Figure 5. Modulation of the Transcriptional Activity of LHW by SACL Proteins

(A) Yeast two-hybrid assays with the four SACL proteins fused to the GAL4 activation domain (AD) and LHW fused to the GAL4 binding domain (BD). Selection was performed in medium lacking histidine and supplied with 20 mM 3-AT to avoid LHW-BD auto-activation.

(B) Average fluorescence lifetime (in nanoseconds) analysis for quantification of FRET measured by FLIM demonstrates direct interaction between SACL3-sCFP3A and LHW-sYFP2. IAA10-YFP was used as a negative control. Means ± SD are represented, and different letters show significantly different means (Tukey's HSD, $p < 0.05$).

(C) Transactivation assay of *LOG4* by LHW and TMO5 in agroinfiltrated *Nicotiana benthamiana* leaves, showing the repression caused by increasing amounts of co-infiltrated SACL3 and the competition with TMO5. Values represent the relative activity of firefly luciferase under the control of the *LOG4* promoter versus the control *Renilla* luciferase and are the average of three technical replicates in one of the three experiments performed. The numbers at the bottom correspond to the relative levels of each of the co-infiltrated genes. Means ± SD are represented, and different letters show significantly different means (Tukey's HSD, $p < 0.05$).

(D) Heatmap summarizing the expression changes (induction in red, repression in blue) of the genes induced in *acl5* but corrected in any of the conditions with increased SACL3 activity. The first row has dye swap data.

are specified to reach proper organ width. Here we identify a mechanism that limits width-increasing periclinal divisions in the vascular tissues. Two pathways have been shown previously to control the radial growth of the vascular tissues. The TMO5/LHW bHLH dimer promotes local CK biosynthesis that controls periclinal divisions in neighboring cells (De Rybel et al., 2014; Ohashi-Ito et al., 2014), whereas the thermospermine synthase ACL5 is required to limit stem vascular tissue expansion (Muñiz et al., 2008). Here we show that these two pathways are molecularly linked. ACL5 promotes the translation of SACL proteins that are able to bind to LHW and act as negative regulators of TMO5/LHW dimer activity. Interestingly, although *ACL5* is conserved in the whole plant kingdom (Minguet et al., 2008), the *TMO5*, *LHW*, and *SACL* clades are conserved in the tracheophyte lineage (Figure S3), suggesting that this regulatory module may be intrinsically linked to the origin of vascular tissues.

TMO5, *LHW*, and *ACL5* are all expressed in the xylem cells of the vascular bundle (De Rybel et al., 2013; Muñiz et al., 2008; Ohashi-Ito and Bergmann, 2007). The fact that *SACL* genes appear biochemically similar and that they show specific expression patterns in the vascular bundle (whole bundle, xylem, protophloem, mostly cambium) provides a mechanism to control cell

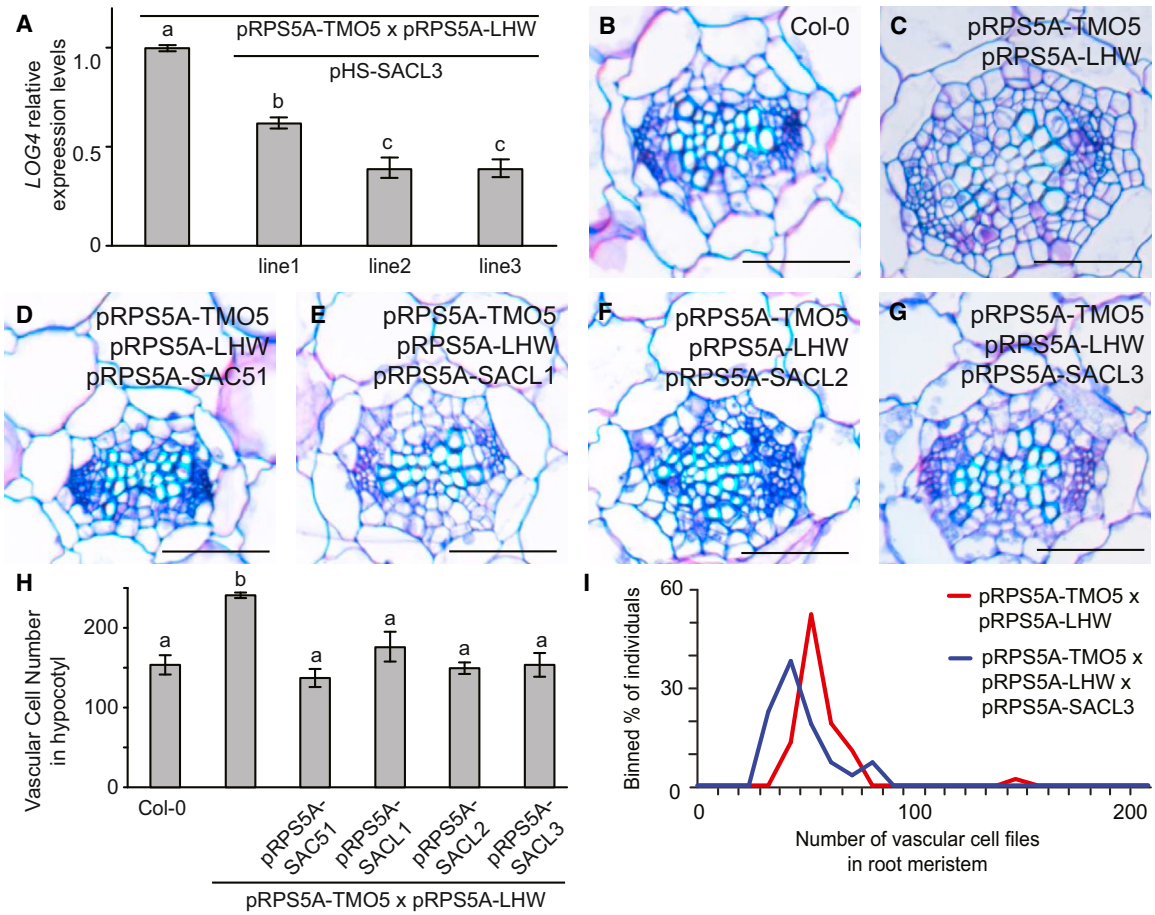

Figure 6. Suppression by *SACL3* of the Vasculature-Related Defects Caused by TMO5/LHW Overexpression

(A) Expression levels of *LOG4* in pRPS5A::TMO5 pRPS5A::LHW with or without pHS::*SACL3*. Ten-day-old seedlings were exposed to 37°C for 30 min, and samples were collected 3 hr and 30 min after heat shock. Three independent lines are shown with reduction in *LOG4* expression levels. Means ± SD are represented, and different letters show significantly different means (Tukey's HSD, $p < 0.05$).

(B–G) Representative sections of 12-day-old hypocotyls in pRPS5A::TMO5 pRPS5A::LHW pRPS5A::SACL (D, SAC51; E, SACL1; F, SACL2; G, SACL3) compared with the Col-0 control (B) and pRPS5A::TMO5 pRPS5A-LHW (C). Scale bars, 100 μm.

(H) Number of cells within the vascular cylinder of the hypocotyls of 12-day-old seedlings. Means ± SD are represented, and different letters show significantly different means (Tukey's HSD, $p < 0.05$).

(I) Quantification of the distribution of vascular cell file number in roots of the indicated lines.

divisions on a tissue-specific level. However, if SACL proteins act only on TMO5/LHW dimer activity, then this also suggests that this feedback control mechanism does not act outside of the xylem domain. However, the broader expression of *LHW* (De Rybel et al., 2013; Ohashi-Ito and Bergmann, 2007) and its negative regulators (*SACL* genes) within the vascular tissues raises the interesting possibility that LHW has still unknown functions outside the xylem domain. Likewise, the *acl5* mutant shows defects that are not induced by *TMO5/LHW* misexpression. For example, *acl5* lacks specific cell types like metaxylem and fiber elements (Muñiz et al., 2008). Moreover, *acl5* also shows early vascular differentiation and cell death (Muñiz et al., 2008). This opens up the possibility that ACL5 and SACL could also modulate the activity of other transcription factor modules besides the TMO5/LHW module. Systematic screening for transcription factors interacting with the SACL proteins should help resolve this question.

Excess TMO5/LHW activity results in massive over-proliferation, whereas loss of function results in a reduction of periclinal cell divisions (De Rybel et al., 2013; Ohashi-Ito and Bergmann, 2007; Ohashi-Ito et al., 2013). Strict control of TMO5/LHW activity in space and time is therefore crucial for normal development. Perhaps not surprisingly, control of TMO5/LHW activity appears to be multifaceted. First, auxin triggers an incoherent feedforward loop by inducing both *TMO5* (Schlereth et al., 2010) and its corresponding *ACL5*-dependent repressing module (Hanzawa et al., 2000). Part of this regulation could be exerted via ATHB8 as described previously (Baima et al., 2014). Second, thermospermine synthesized by ACL5 inhibits the translational repression of SAC51 (Imai et al., 2006; Takano et al., 2012) and, presumably, other SACL proteins, therefore increasing their protein levels. Third, SACL proteins interact with LHW and inhibit the activity of the TMO5/LHW dimer. Given that no interactions could be detected between TMO5 and SACL proteins

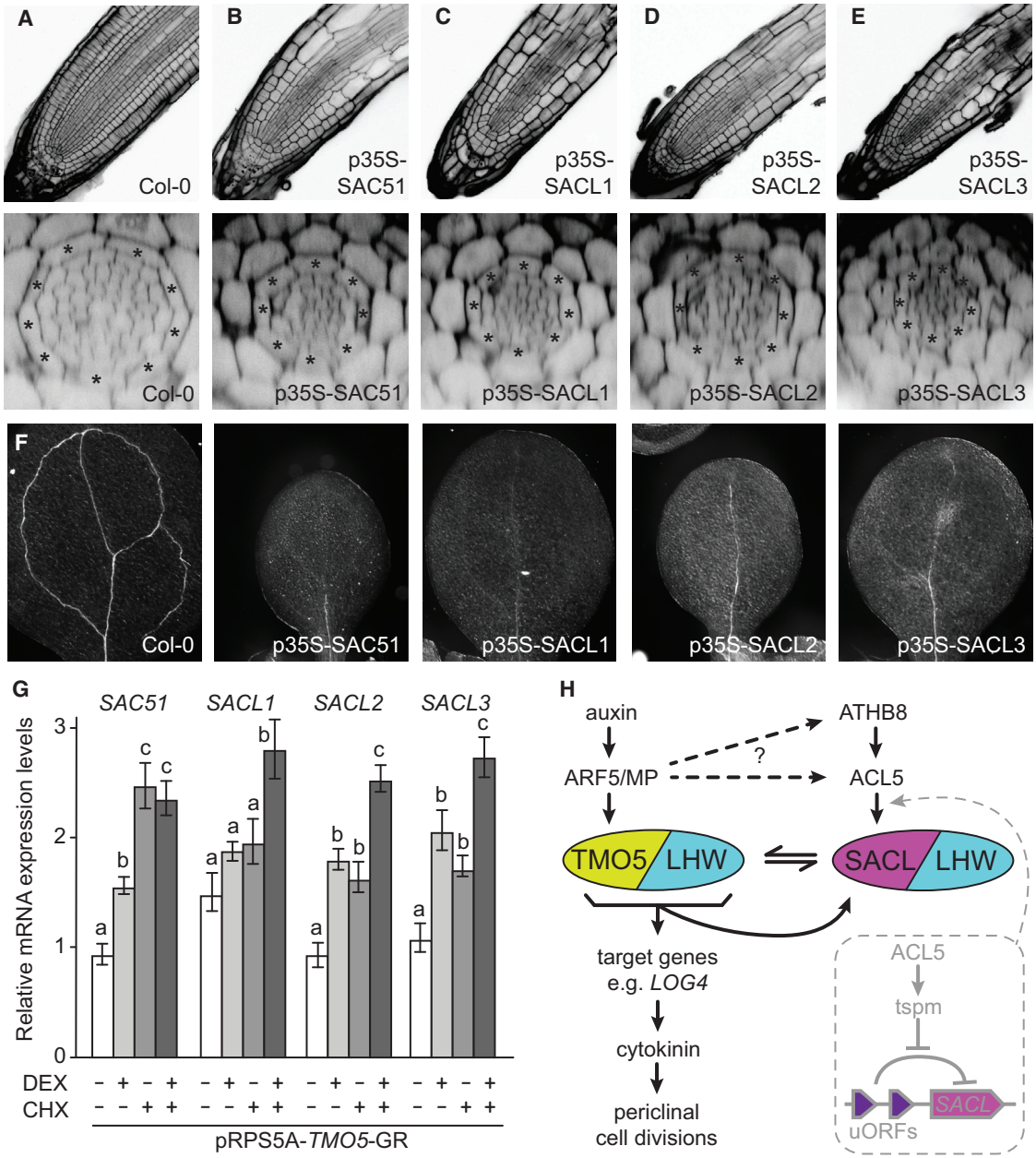

Figure 7. *SACL* Overexpression Reduces Cell Division during Vascular Development

(A–E) Images of representative roots (top row) and reconstruction of optical cross-sections (bottom row) showing the reduction in cell number in p35S::*SACL* lines (B, SAC51; C, SACL1; D, SACL2; E, SACL3) relative to the wild-type (A). Asterisks indicate endodermal cells.

(F) Defective vasculature in the cotyledons of the same lines.

(G) Relative expression levels of the four *SACL* genes in pRPS5A::*TMO5*:GR treated with mock (control), 10 μM dexamethasone (DEX), 10 μM cycloheximide (CHX), or a combination of CHX and DEX for 1 hr. Bars represent SE. Means ± SD are represented, and different letters show significantly different means (Tukey's HSD, $p < 0.05$).

(H) Model representing the proposed interaction network in which the ACL5/SACL module controls TMO5/LHW-dependent vascular cell proliferation.

in IP-MS/MS (De Rybel et al., 2013), it is plausible that SACL proteins are competitive inhibitors that displace TMO5 in the TMO5/LHW complex. Irrespective of the exact mode of inhibition, the thermospermine-SACL pathway suppresses vascular periclinal divisions. At the same time, TMO5/LHW promotes the expression of *SACL* genes, likely by direct activation of their promoters. Therefore, this transcription complex activates its own inhibitor, forming a dedicated negative feedback module. Similar feedback modules operate in several hormone signaling pathways. For example, the AUXIN RESPONSE FACTORS (ARFs) activate the expression of Aux/IAA genes, whose protein products bind to and inhibit the ARFs, therefore limiting transcriptional output

after an initial auxin response (Reed, 2001). It appears that the two negative regulatory mechanisms that control activity of the TMO5/LHW dimer are potentially linked. In poplar, the ACL5 ortholog suppressed auxin accumulation, whereas auxin promoted *ACL5* expression (Milhinhos et al., 2013). Likewise, because the auxin-dependent *TMO5* and *T5L1* transcripts are upregulated in the *acl5* mutant (Figure 1E), a similar mode of regulation might act in *Arabidopsis*. Furthermore, because *TMO5* and *ACL5* expression are direct outputs of MONOPTEROS (MP) and auxin response (Schlereth et al., 2010) and loss of MP function is largely epistatic over *acl5* (Tong et al., 2014), there are likely intricate connections between transcriptional and translational control in this pathway. However, precise quantitative analysis and perhaps modeling will be required to understand the dynamics of this system.

The network identified here accounts for the quantitative control of vascular tissues in the root, hypocotyl, and leaf, which are all the result of primary vascular tissue development. However, in *Arabidopsis* as in other species, vascular tissues can undergo dramatic increases in width upon activation of vascular cambium during secondary growth (Etchells et al., 2015). Several genetic regulators of secondary growth have been identified and ordered in networks (Fisher and Turner, 2007; Hirakawa et al., 2008, 2010; Ito et al., 2006). At present, there is no strong indication that factors controlling secondary growth in *Arabidopsis* likely act in primary vascular tissue development. However, it is possible that the basic modules for promoting periclinal cell division are re-activated during secondary growth. It will therefore be interesting to determine which parts of the network described here are recruited to quantitatively control vascular tissue growth during secondary growth.

EXPERIMENTAL PROCEDURES

Plant Material and Treatments

All seeds were surface-sterilized, sown on solid MS plates, and stratified for 2 days before growing at a constant temperature of 22°C in a growth room. *Arabidopsis thaliana* mutants are listed in the Supplemental Experimental Procedures. Dexamethasone and cycloheximide treatments were performed as described previously (De Rybel et al., 2013). *Trans*-zeatin and N6-benzyladenine treatments were performed as described previously (Marín-de la Rosa et al., 2015).

Microscopic Analysis

The cleared leaf histological analysis was performed as described previously (Sieburth, 1999). For paraffin transverse sections, leaves were fixed in PBS containing 4% paraformaldehyde by vacuum infiltration for 5 min. Samples were dehydrated in consecutive ethanol solutions up to 70% ethanol. Samples were embedded in paraffin using a Leica TP1020 tissue processor. Sections were cut in a Microm microtome, stained with toluidine blue at 0.02%, and observed with a Nikon Eclipse E600 microscope. For the thin-resin hypocotyl sections, histological procedures were as described previously (Carbonell-Bejerano et al., 2010). For the root basic fuchsin staining, roots from 4-day-old seedlings were stained as described previously (Mähönen et al., 2000). Roots were analyzed under a Zeiss AX10 confocal microscope. All photos were taken from 0.75 mm of the hypocotyl-root limit. For the hypocotyl localization of the p*SACL*-n3GFP, p*TMO5*-n3GFP, and p*LHW*-n3GFP reporters, 4-day-old etiolated seedlings were analyzed under a Leica TCS SL confocal microscope. The root and embryo localization of p*SACL*-n3GFP was performed as described previously (Llavata-Peris et al., 2013) using a Leica SP5 system with hybrid detectors. The localization of SACL, TMO5, and LHW in *Nicotiana benthamiana* leaves was performed as described previously (Locascio et al., 2013).

qRT-PCR Analysis

qRT-PCR analyses and primers are described in detail in the Supplemental Experimental Procedures.

Mapping of *ajax* Suppressor Mutants

The screening, mapping, and cloning of *ajax/sacl* suppressors are described in detail in the Supplemental Experimental Procedures.

Cloning and Constructs

All constructs and primers used in this study are summarized in the Supplemental Experimental Procedures.

In Vitro Transcription-Translation

For the in vitro transcription, 10 μg of the pSP64 plasmid was linearized with EcoRI, and the transcription reaction was performed with 3 μg of linearized plasmid, 20 units of SP6 RNA polymerase (Roche); 20 units of RNase inhibitor (Roche); 2 μl of 10× buffer; and 0.5 mm ATP, guanosine triphosphate (GTP), cytidine triphosphate (CTP), and uridine triphosphate (UTP). The reaction mixture was incubated for 2 hr at 37°C. 20 units of DNaseI (Roche) were added and incubated for 30 min at 37°C.

In vitro translation was performed with 12 μg of RNA, 12 μl of Wheat Germ Extract Plus (Promega), and 0.5 μl of Fluorotect Green Lys tRNA (Promega). The reaction mixture was incubated for 2 hr at 25°C. The products were separated by SDS-PAGE in a 12% acrylamide gel, which was scanned using a Typhoon TRIO (Amersham Biosciences).

Alignment and Phylogenetic Analysis

All sequences used in this study are summarized in Table S3. They were obtained from previous work (Hayden and Jorgensen, 2007; Pires and Dolan, 2010; Toledo-Ortiz et al., 2003) or found by BLAST analysis using the uORFS and the main ORF of the *Arabidopsis SACL* genes as baits in the NCBI (http://www.ncbi.nlm.nih.gov) and Phytozome (http://www.phytozome.net) databases. The alignment of the sequences was done with CLUSTALX software (Thompson et al., 1997), and the phylogenetic tree was constructed with FigTree software (http://tree.bio.ed.ac.uk/software/figtree/). The different subfamilies of bHLH were divided based on previous studies (Pires and Dolan, 2010).

Yeast Two-Hybrid Assays

The ORFs of *SAC51*, *SACL1*, *SACL2*, and *SACL3* were fused to the GAL4 activation domain by cloning them into pDEST22 (Invitrogen), and the ORFs of *LHW* were fused to the GAL4 binding domain by cloning them into pDEST32 (Invitrogen). Assays were performed in the yeast strain AH109 (Clontech Laboratories). Yeasts were tested for interactions in synthetic dextrose/-Leu/-Trp/-His medium plus 3-amino-1,2,4-triazole (3-AT).

Protein Extraction and Western Blot

Protein extraction and western blot analysis were performed as reported previously (Alabadí et al., 2008).

Transcript Profiling and Data Analysis

Microarray data have been deposited in the NCBI's GEO (Edgar et al., 2002) and are accessible through GEO series accession number GSE70157 (http://www.ncbi.nlm.nih.gov/geo/query/acc.cgi?acc=GSE70157). More information is available in the Supplemental Experimental Procedures.

FRET-FLIM

FRET-FLIM analysis in *Arabidopsis* leaf mesophyll protoplasts was performed as described previously (Bücherl et al., 2013; De Rybel et al., 2013) with minor modifications. Details are described in the Supplemental Experimental Procedures.

Nicotiana benthamiana Transcriptional Assays

The ORFs of *LHW* and *TMO5* were cloned into the pEarlyGate 201 vector, and the *SACL3* ORF was cloned into pEarlyGate 104. All of these construct were inserted into *Agrobacterium tumefaciens* C58 cells. The reporter line pGreenII 0800 + *LOG4* promoter was inserted into *Agrobacterium tumefaciens* C58 + pSOUP cells. All transient expression assays were performed as described previously (Marín-de la Rosa et al., 2014).

Statistical Analysis

To ensure the existence of significant differences between the averages of the different samples, one-way ANOVA was performed for each experiment, discarding the null hypothesis (the means of all samples are equal). To define the differences between different samples, a post hoc Tukey honest significant difference (HSD) pairwise comparison was done. All calculations were done at http://statistica.mooo.com/OneWay_Anova_with_TukeyHSD, except for data in Figure 5C (with more than the ten maximum treatments accepted by the web page), for which the calculations were done in an Excel tab following the instructions from the same web page. All raw data and statistical analysis are available in Table S4.

ACCESSION NUMBERS

The accession number for the microarray data reported in this paper is GEO: GSE70157.

SUPPLEMENTAL INFORMATION

Supplemental Information includes Supplemental Experimental Procedures, seven figures, and four tables and can be found with this article online at http://dx.doi.org/10.1016/j.devcel.2015.10.022.

AUTHOR CONTRIBUTIONS

Conceptualization, B.D.R., D.W., F.V.S., and M.A.B.; Formal Analysis, B.D.R. and F.V.S.; Investigation, B.D.R., C.U., E.G.M., E.K., F.V.S., J.C.A.M., J.W.B., and M.P.; Writing – Original Draft, B.D.R., D.W., F.V.S., and M.A.B.; Writing – Review & Editing, B.D.R., D.W., F.V.S., H.T., J.C., and M.A.B.; Supervision, D.W. and M.A.B.

ACKNOWLEDGMENTS

The authors would like to thank the genetic mapping facility at Miguel Hernández University (Elche) run by José L. Micol and María Rosa Ponce and the microscopy service of the Universidad Politécnica of Valencia. We also thank J. Agustí, D. Alabadí, D. Esteve, C. Ferrándiz, M. de Lucas, and F. Madueño for discussions and critical reading of the manuscript. B.D.R. was funded by long-term FEBS and Marie Curie (IEF-2009-252503) Fellowships, the Netherlands Organization for Scientific Research (NWO VIDI 864.13.001), and by the Research Foundation Flanders (FWO G0D0515N and 12D1815N). D.W. was funded by the Netherlands Organization for Scientific Research (ERA-CAPS project EURO-PEC, 849.13.006) and the European Research Council (Starting Grant "CELLPATTERN," contract no. 281573). M.P. was funded by La Caixa fellowship. J.C. was the recipient of grant BIO2011-23828 from the Spanish Ministry of Science and Innovation.

Received: July 8, 2015
Revised: October 5, 2015
Accepted: October 23, 2015
Published: November 23, 2015

REFERENCES

Alabadí, D., Gallego-Bartolomé, J., Orlando, L., García-Cárcel, L., Rubio, V., Martínez, C., Frigerio, M., Iglesias-Pedraz, J.M., Espinosa, A., Deng, X.W., and Blázquez, M.A. (2008). Gibberellins modulate light signaling pathways to prevent Arabidopsis seedling de-etiolation in darkness. Plant J. *53*, 324–335.

Baima, S., Forte, V., Possenti, M., Peñalosa, A., Leoni, G., Salvi, S., Felici, B., Ruberti, I., and Morelli, G. (2014). Negative feedback regulation of auxin signaling by ATHB8/ACL5-BUD2 transcription module. Mol. Plant *7*, 1006–1025.

Bücherl, C.A., van Esse, G.W., Kruis, A., Luchtenberg, J., Westphal, A.H., Aker, J., van Hoek, A., Albrecht, C., Borst, J.W., and de Vries, S.C. (2013). Visualization of BRI1 and BAK1(SERK3) membrane receptor heterooligomers during brassinosteroid signaling. Plant Physiol. *162*, 1911–1925.

Carbonell-Bejerano, P., Urbez, C., Carbonell, J., Granell, A., and Perez-Amador, M.A. (2010). A fertilization-independent developmental program triggers partial fruit development and senescence processes in pistils of Arabidopsis. Plant Physiol. *154*, 163–172.

Chickarmane, V.S., Gordon, S.P., Tarr, P.T., Heisler, M.G., and Meyerowitz, E.M. (2012). Cytokinin signaling as a positional cue for patterning the apical-basal axis of the growing Arabidopsis shoot meristem. Proc. Natl. Acad. Sci. USA *109*, 4002–4007.

Clay, N.K., and Nelson, T. (2005). Arabidopsis thickvein mutation affects vein thickness and organ vascularization, and resides in a provascular cell-specific spermine synthase involved in vein definition and in polar auxin transport. Plant Physiol. *138*, 767–777.

De Rybel, B., Möller, B., Yoshida, S., Grabowicz, I., Barbier de Reuille, P., Boeren, S., Smith, R.S., Borst, J.W., and Weijers, D. (2013). A bHLH complex controls embryonic vascular tissue establishment and indeterminate growth in Arabidopsis. Dev. Cell *24*, 426–437.

De Rybel, B., Adibi, M., Breda, A.S., Wendrich, J.R., Smit, M.E., Novák, O., Yamaguchi, N., Yoshida, S., Van Isterdael, G., Palovaara, J., et al. (2014). Plant development. Integration of growth and patterning during vascular tissue formation in Arabidopsis. Science *345*, 1255215.

Edgar, R., Domrachev, M., and Lash, A.E. (2002). Gene Expression Omnibus: NCBI gene expression and hybridization array data repository. Nucleic Acids Res. *30*, 207–210.

Etchells, J.P., Mishra, L.S., Kumar, M., Campbell, L., and Turner, S.R. (2015). Wood Formation in Trees Is Increased by Manipulating PXY-Regulated Cell Division. Curr. Biol. *25*, 1050–1055.

Fisher, K., and Turner, S. (2007). PXY, a receptor-like kinase essential for maintaining polarity during plant vascular-tissue development. Curr. Biol. *17*, 1061–1066.

Hanzawa, Y., Takahashi, T., and Komeda, Y. (1997). ACL5: an Arabidopsis gene required for internodal elongation after flowering. Plant J. *12*, 863–874.

Hanzawa, Y., Takahashi, T., Michael, A.J., Burtin, D., Long, D., Pineiro, M., Coupland, G., and Komeda, Y. (2000). ACAULIS5, an Arabidopsis gene required for stem elongation, encodes a spermine synthase. EMBO J. *19*, 4248–4256.

Hayden, C.A., and Jorgensen, R.A. (2007). Identification of novel conserved peptide uORF homology groups in Arabidopsis and rice reveals ancient eukaryotic origin of select groups and preferential association with transcription factor-encoding genes. BMC Biol. *5*, 32.

Hirakawa, Y., Shinohara, H., Kondo, Y., Inoue, A., Nakanomyo, I., Ogawa, M., Sawa, S., Ohashi-Ito, K., Matsubayashi, Y., and Fukuda, H. (2008). Non-cell-autonomous control of vascular stem cell fate by a CLE peptide/receptor system. Proc. Natl. Acad. Sci. USA *105*, 15208–15213.

Hirakawa, Y., Kondo, Y., and Fukuda, H. (2010). TDIF peptide signaling regulates vascular stem cell proliferation via the WOX4 homeobox gene in Arabidopsis. Plant Cell *22*, 2618–2629.

Imai, A., Hanzawa, Y., Komura, M., Yamamoto, K.T., Komeda, Y., and Takahashi, T. (2006). The dwarf phenotype of the Arabidopsis acl5 mutant is suppressed by a mutation in an upstream ORF of a bHLH gene. Development *133*, 3575–3585.

Imai, A., Komura, M., Kawano, E., Kuwashiro, Y., and Takahashi, T. (2008). A semi-dominant mutation in the ribosomal protein L10 gene suppresses the dwarf phenotype of the acl5 mutant in Arabidopsis thaliana. Plant J. *56*, 881–890.

Ito, Y., Nakanomyo, I., Motose, H., Iwamoto, K., Sawa, S., Dohmae, N., and Fukuda, H. (2006). Dodeca-CLE peptides as suppressors of plant stem cell differentiation. Science *313*, 842–845.

Jouannet, V., Brackmann, K., and Greb, T. (2015). (Pro)cambium formation and proliferation: two sides of the same coin? Curr. Opin. Plant Biol. *23*, 54–60.

Kakehi, J., Kuwashiro, Y., Motose, H., Igarashi, K., and Takahashi, T. (2010). Norspermine substitutes for thermospermine in the control of stem elongation in Arabidopsis thaliana. FEBS Lett. *584*, 3042–3046.

Kakehi, J., Kawano, E., Yoshimoto, K., Cai, Q., Imai, A., and Takahashi, T. (2015). Mutations in ribosomal proteins, RPL4 and RACK1, suppress the

phenotype of a thermospermine-deficient mutant of Arabidopsis thaliana. PLoS ONE *10*, e0117309.

Knott, J.M., Römer, P., and Sumper, M. (2007). Putative spermine synthases from Thalassiosira pseudonana and Arabidopsis thaliana synthesize thermospermine rather than spermine. FEBS Lett. *581*, 3081–3086.

Llavata-Peris, C., Lokerse, A., Möller, B., De Rybel, B., and Weijers, D. (2013). Imaging of phenotypes, gene expression, and protein localization during embryonic root formation in Arabidopsis. Methods Mol. Biol. *959*, 137–148.

Locascio, A., Blázquez, M.A., and Alabadí, D. (2013). Dynamic regulation of cortical microtubule organization through prefoldin-DELLA interaction. Curr. Biol. *23*, 804–809.

Lucas, W.J., Groover, A., Lichtenberger, R., Furuta, K., Yadav, S.-R., Helariutta, Y., He, X.-Q., Fukuda, H., Kang, J., Brady, S.M., et al. (2013). The plant vascular system: evolution, development and functions. J. Integr. Plant Biol. *55*, 294–388.

Mähönen, A.P., Bonke, M., Kauppinen, L., Riikonen, M., Benfey, P.N., and Helariutta, Y. (2000). A novel two-component hybrid molecule regulates vascular morphogenesis of the Arabidopsis root. Genes Dev. *14*, 2938–2943.

Mähönen, A.P., Bishopp, A., Higuchi, M., Nieminen, K.M., Kinoshita, K., Törmäkangas, K., Ikeda, Y., Oka, A., Kakimoto, T., and Helariutta, Y. (2006). Cytokinin signaling and its inhibitor AHP6 regulate cell fate during vascular development. Science *311*, 94–98.

Marín-de la Rosa, N., Sotillo, B., Miskolczi, P., Gibbs, D.J., Vicente, J., Carbonero, P., Oñate-Sánchez, L., Holdsworth, M.J., Bhalerao, R., Alabadí, D., and Blázquez, M.A. (2014). Large-scale identification of gibberellin-related transcription factors defines group VII ETHYLENE RESPONSE FACTORS as functional DELLA partners. Plant Physiol. *166*, 1022–1032.

Marín-de la Rosa, N., Pfeiffer, A., Hill, K., Locascio, A., Bhalerao, R.P., Miskolczi, P., Grønlund, A.L., Wanchoo-Kohli, A., Thomas, S.G., Bennett, M.J., et al. (2015). Genome Wide Binding Site Analysis Reveals Transcriptional Coactivation of Cytokinin-Responsive Genes by DELLA Proteins. PLoS Genet. *11*, e1005337.

Matsuhara, S., Jingu, F., Takahashi, T., and Komeda, Y. (2000). Heat-shock tagging: a simple method for expression and isolation of plant genome DNA flanked by T-DNA insertions. Plant J. *22*, 79–86.

Milhinhos, A., Prestele, J., Bollhöner, B., Matos, A., Vera-Sirera, F., Rambla, J.L., Ljung, K., Carbonell, J., Blázquez, M.A., Tuominen, H., and Miguel, C.M. (2013). Thermospermine levels are controlled by an auxin-dependent feedback loop mechanism in Populus xylem. Plant J. *75*, 685–698.

Minguet, E.G., Vera-Sirera, F., Marina, A., Carbonell, J., and Blázquez, M.A. (2008). Evolutionary diversification in polyamine biosynthesis. Mol. Biol. Evol. *25*, 2119–2128.

Muñiz, L., Minguet, E.G., Singh, S.K., Pesquet, E., Vera-Sirera, F., Moreau-Courtois, C.L., Carbonell, J., Blázquez, M.A., and Tuominen, H. (2008). ACAULIS5 controls Arabidopsis xylem specification through the prevention of premature cell death. Development *135*, 2573–2582.

Nieminen, K., Blomster, T., Helariutta, Y., and Mähönen, A.P. (2015). Vascular Cambium Development. Arabidopsis Book *13*, e0177.

Ohashi-Ito, K., and Bergmann, D.C. (2007). Regulation of the Arabidopsis root vascular initial population by LONESOME HIGHWAY. Development *134*, 2959–2968.

Ohashi-Ito, K., Matsukawa, M., and Fukuda, H. (2013). An atypical bHLH transcription factor regulates early xylem development downstream of auxin. Plant Cell Physiol. *54*, 398–405.

Ohashi-Ito, K., Saegusa, M., Iwamoto, K., Oda, Y., Katayama, H., Kojima, M., Sakakibara, H., and Fukuda, H. (2014). A bHLH complex activates vascular cell division via cytokinin action in root apical meristem. Curr. Biol. *24*, 2053–2058.

Pires, N., and Dolan, L. (2010). Origin and diversification of basic-helix-loop-helix proteins in plants. Mol. Biol. Evol. *27*, 862–874.

Reed, J.W. (2001). Roles and activities of Aux/IAA proteins in Arabidopsis. Trends Plant Sci. *6*, 420–425.

Schlereth, A., Möller, B., Liu, W., Kientz, M., Flipse, J., Rademacher, E.H., Schmid, M., Jürgens, G., and Weijers, D. (2010). MONOPTEROS controls embryonic root initiation by regulating a mobile transcription factor. Nature *464*, 913–916.

Sieburth, L.E. (1999). Auxin is required for leaf vein pattern in Arabidopsis. Plant Physiol. *121*, 1179–1190.

Takano, A., Kakehi, J., and Takahashi, T. (2012). Thermospermine is not a minor polyamine in the plant kingdom. Plant Cell Physiol. *53*, 606–616.

Thompson, J.D., Gibson, T.J., Plewniak, F., Jeanmougin, F., and Higgins, D.G. (1997). The CLUSTAL_X windows interface: flexible strategies for multiple sequence alignment aided by quality analysis tools. Nucleic Acids Res. *25*, 4876–4882.

Tokunaga, H., Kojima, M., Kuroha, T., Ishida, T., Sugimoto, K., Kiba, T., and Sakakibara, H. (2012). Arabidopsis lonely guy (LOG) multiple mutants reveal a central role of the LOG-dependent pathway in cytokinin activation. Plant J. *69*, 355–365.

Toledo-Ortiz, G., Huq, E., and Quail, P.H. (2003). The Arabidopsis basic/helix-loop-helix transcription factor family. Plant Cell *15*, 1749–1770.

Tong, W., Yoshimoto, K., Kakehi, J., Motose, H., Niitsu, M., and Takahashi, T. (2014). Thermospermine modulates expression of auxin-related genes in Arabidopsis. Front. Plant Sci. *5*, 94.